Inorganic Chemistry

pubs.acs.org/IC

Article

C(sp)−H, S−H, and Sn−H Bond Activation with a Cobalt(I) Pincer Complex

Sayantani Saha, Jeanette A. Krause, and Hairong Guan*

Cite This: *Inorg. Chem.* 2024, 63, 13689−13699

Read Online

ACCESS | Metrics & More | Article Recommendations | Supporting Information

ABSTRACT: This study focuses on the stoichiometric reactions of {2,6-(^{i}Pr$_2$PO)$_2$C$_6$H$_3$}-Co(PMe$_3$)$_2$ with terminal alkynes, thiols, and tin hydrides as part of an effort to develop catalytic, two-electron processes with cobalt. This specific Co(I) pincer complex proves to be effective for cleaving the C(sp)−H, S−H, and Sn−H bonds to give oxidative addition products with the general formula {2,6-(^{i}Pr$_2$PO)$_2$C$_6$H$_3$}CoHX(PMe$_3$) (X = alkynyl, thiolate, and stannyl groups) along with the free PMe$_3$. These reactions typically reach completion when the substituents on acetylene, sulfur, and tin are electron-withdrawing groups (e.g., phenyl, pyridyl, and alkenyl groups). In contrast, alkyl-substituted acetylenes, 1-pentanethiol, and tributyltin hydride are partially converted due to the equilibria with the corresponding oxidative addition products. The Co(I) pincer complex is not a hydrothiolation catalyst but capable of catalyzing the hydrostannation of terminal alkynes with Ph$_3$SnH to produce β-(*Z*)-alkenylstannanes selectively.

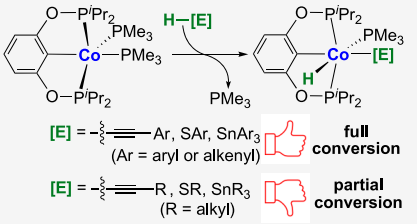

INTRODUCTION

Oxidative addition and reductive elimination are fundamentally important steps that are frequently proposed in transition metal-catalyzed organic transformations. When a single metal is tasked to perform these reactions, the metal center is formally oxidized or reduced by two electrons, which poses considerable challenges for first-row transition metals due to their tendency to undergo one-electron redox processes. Strategies to bypass the obstacles are thus being developed, including the design of redox-active ligands[1] or the incorporation of a second metal,[2] to assist in electron transfer.

Strong-field ligands, in principle, can widen the energy gaps between d orbitals to the extent that first-row transition metals may display reactivity akin to their second and third row counterparts. Guided by this hypothesis, we have been interested in synthesizing cobalt complexes with pincer ligands of the type [2,6-(R$_2$PO)$_2$C$_6$H$_3$]$^-$,[3] in which a strongly σ-donating phenyl group is flanked by two phosphorus donors. This specific pincer ligand system has proven to be successful in developing rhodium-catalyzed C−S coupling reactions[4] and iridium-catalyzed transfer dehydrogenation reactions,[5] all involving a M(I)/M(III) catalytic cycle.

The seminal work by Heinekey has established the ability of {2,6-(^{t}Bu$_2$PO)$_2$C$_6$H$_3$}Co(H$_2$) to participate in an oxidative addition reaction with H$_2$, although the product is stable only below −53 °C (eq 1).[6] It is worth noting that {2,6-(^{t}Bu$_2$PO)$_2$C$_6$H$_3$}Co(H$_2$) is a diamagnetic compound. Without H$_2$ acting as an ancillary ligand, the {2,6-(^{t}Bu$_2$PO)$_2$C$_6$H$_3$}Co fragment itself prefers a triplet ground state (S = 1, based on DFT calculations).[6] The analogous {2,6-(^{t}Bu$_2$PO)$_2$C$_6$H$_3$}Ir, however, adopts the singlet electronic configuration (S = 0).[7] For an example of reductive elimination reactions, the Ozerov group has shown that {2,6-(^{i}Pr$_2$PO)$_2$C$_6$H$_3$}CoPh(SPh) undergoes aryl−aryl elimination, which is accompanied by one-electron processes (eq 2).[8] In contrast, the rhodium analog, {2,6-(^{i}Pr$_2$PO)$_2$C$_6$H$_3$}RhPh(SPh), reductively eliminates diphenyl sulfide to yield {2,6-(^{i}Pr$_2$PO)$_2$C$_6$H$_3$}Rh(SPh$_2$) as the sole product.[4] These results seem to support the notion that the [2,6-(R$_2$PO)$_2$C$_6$H$_3$]$^-$ ligand platform alone is inadequate to force a low-spin state for cobalt while promoting precious-metal-like reactivity (i.e., clean two-electron processes).[9] The presence of another ligand, abbreviated as L, may render {2,6-(R$_2$PO)$_2$C$_6$H$_3$}Co(L) diamagnetic and ultimately feasible for a Co(I)/Co(III) catalytic cycle.

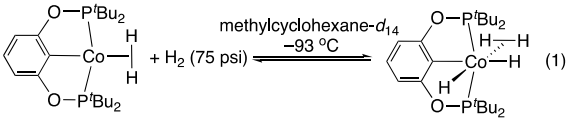

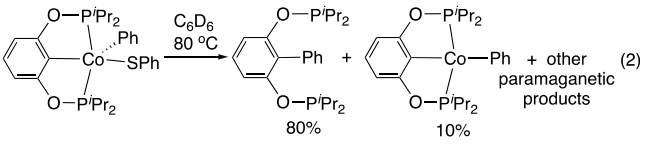

In a recent report, we have demonstrated oxidative addition of silanes such as PhSiH$_3$ to {2,6-(^{i}Pr$_2$PO)$_2$C$_6$H$_3$}Co(PMe$_3$)$_2$ to form a Co(III) hydride species and free PMe$_3$ (eq 3).[3b] These reactions are reversible, likely proceeding via the 4-

Received: May 14, 2024
Revised: June 15, 2024
Accepted: June 20, 2024
Published: July 8, 2024

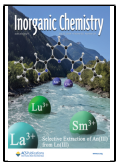

coordinate, diamagnetic intermediate {2,6-(^{i}Pr$_2$PO)$_2$C$_6$H$_3$}Co(PMe$_3$). In a closely related study, Li and coworkers have shown that {1,3-(Ph$_2$PO)$_2$C$_3$H$_5$}Co(PMe$_3$)$_2$ reacts with iodomethane following an oxidative addition pathway (eq 4).[10] Taken together, these examples suggest that the combination of a bis(phosphinite)-type (or POCOP-type) pincer ligand and PMe$_3$ can direct cobalt to undergo two-electron processes. The work presented herein reinforces the effectiveness of this strategy. More specifically, substrates for {2,6-(^{i}Pr$_2$PO)$_2$C$_6$H$_3$}Co(PMe$_3$)$_2$ are now expanded to molecules bearing other oxidatively cleavable bonds such as terminal alkynes (C(sp)−H bonds), thiols (S−H bonds), and organotin hydrides (Sn−H bonds). The potential involvement of the oxidative addition products (or lack thereof) in catalytic hydrothiolation and hydrostannation of alkynes is also discussed.

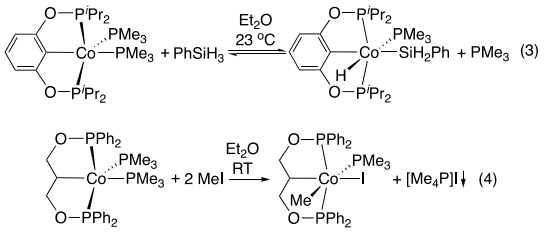

RESULTS AND DISCUSSION

C(sp)−H Oxidative Addition. In recent years, there has been growing interest in developing cobalt-catalyzed C−H bond activation reactions.[11] Understanding how well-defined cobalt complexes cleave various C−H bonds would be useful to guide the design of new catalysts. Of particular note are cobalt aryl complexes, which sometimes can be isolated or spectroscopically observed from the reactions of arenes, presumably involving a C(sp^2)−H bond activation step with[3,12] or without[13] a directing group (DG). The analogous processes with C(sp^3)−H bonds are often intramolecular or DG-promoted.[10,14] There are also examples of cobalt alkynyl complexes obtained from HC≡CR and cobalt species bearing a methyl[13c,15] or hydroxyl group.[16] Most of these Co−C bond forming reactions eliminate H$_2$, CH$_4$, or H$_2$O, which drives the C−H bond activation but complicates the direct analysis of the oxidative addition step. Encouraged by our initial success with Si−H oxidative addition to {2,6-(^{i}Pr$_2$PO)$_2$C$_6$H$_3$}Co(PMe$_3$)$_2$ (eq 3), we were curious to know if this Co(I) pincer complex could also cleave C(sp)−H bonds in terminal alkynes. This type of C(sp)−H oxidative addition reaction has precedent with other low-valent cobalt complexes such as {(Me$_3$P)$_3$CoH}$_2$(N$_2$),[15] [{(Ph$_2$PCH$_2$CH$_2$)$_3$P}Co(N$_2$)]BPh$_4$,[17] and [(Et$_2$PCH$_2$CH$_2$PEt$_2$)$_2$Co(CS$_2$)]BPh$_4$[18] as well as heterobimetallic Zr/Co complexes,[19] although only a limited set of alkynes have been examined.

For this work, phenylacetylene was first chosen as the alkyne to react with {2,6-(^{i}Pr$_2$PO)$_2$C$_6$H$_3$}Co(PMe$_3$)$_2$. The 1:1 reaction carried out at room temperature in C$_6$D$_6$ showed an immediate color change from dark red to light yellow. The ^{1}H NMR spectrum recorded within 15 min of mixing the reagents revealed a characteristic hydride resonance at −12.76 ppm as a doublet of triplets ($^2J_{H-P}$ = 111.6 and 60.8 Hz). The ^{31}P{^{1}H} NMR spectrum displayed two broad resonances at 205.8 ppm and −1.9 ppm (integrate to a 2:1 ratio) and a sharp resonance at −62.6 ppm indicative of free PMe$_3$. The broadening is likely caused by the quadrupolar ^{59}Co nucleus. The NMR data are consistent with a cobalt hydride supported by the pincer ligand and one PMe$_3$ ligand. The most plausible product is {2,6-(^{i}Pr$_2$PO)$_2$C$_6$H$_3$}CoH(C≡CPh)(PMe$_3$) (**1**) resulting from C(sp)−H oxidative addition of phenylacetylene to {2,6-(^{i}Pr$_2$PO)$_2$C$_6$H$_3$}Co(PMe$_3$), which can be generated from {2,6-(^{i}Pr$_2$PO)$_2$C$_6$H$_3$}Co(PMe$_3$)$_2$ via PMe$_3$ dissociation.

Further characterization of **1** was carried out with a purified sample isolated from the reaction of {2,6-(^{i}Pr$_2$PO)$_2$C$_6$H$_3$}Co(PMe$_3$)$_2$ with phenylacetylene in toluene (eq 5). The solid sample exhibited an off-white color, in contrast to the dark red color observed with the starting Co(I) complex. The IR spectrum of **1** (solid sample) contained absorption bands at 2087 and 1977 cm^{-1}, which can be assigned to the C≡C and Co−H stretches, respectively. Spatial arrangement of the ligands around cobalt was more firmly established by X-ray crystallography using single crystals grown from toluene-pentane. As illustrated in Figure 1, the hydride ligand is *trans* to

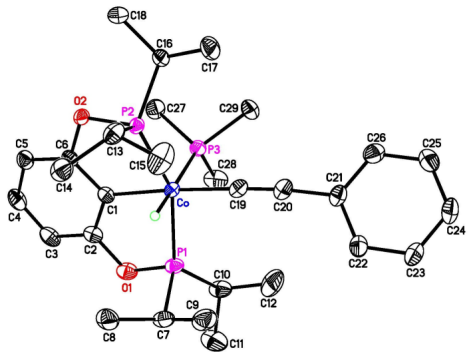

Figure 1. ORTEP of {2,6-(^{i}Pr$_2$PO)$_2$C$_6$H$_3$}CoH(C≡CPh)(PMe$_3$) (**1**) at the 50% probability level (all hydrogen atoms except the one bound to cobalt are omitted for clarity). Selected bond lengths (Å) and angles (deg): Co−C1 1.9358(12), Co−C19 1.9034(13), Co−P1 2.1599(4), Co−P2 2.1529(3), Co−P3 2.2377(4), C19−C20 1.2154(19), Co−H 1.401(18); P1−Co−P2 152.587(15), C1−Co−P3 92.15(4), C1−Co−C19 175.84(5).

PMe$_3$, while the alkynyl group is *trans* to the central donor of the pincer ligand. In C$_6$D$_6$, **1** is thermally stable, provided that it is kept under an inert atmosphere. In fact, heating the solution to 80 °C did not result in any spectral change, implying that this compound is configurationally stable at this temperature.

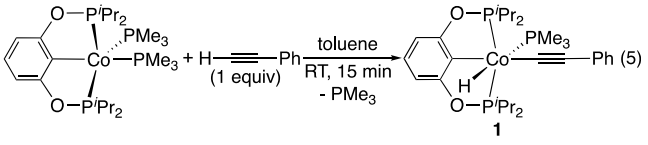

To better understand how the supporting ligands affect the C(sp)−H oxidative addition process, HCo(PMe$_3$)$_4$, a Co(I) complex without a pincer ligand, was treated with 1 equiv of phenylacetylene in C$_6$D$_6$. No net reaction was observed at room temperature. However, at 80 °C, phenylacetylene was fully consumed to give a complicated mixture featuring vinylic hydrogens; HCo(PMe$_3$)$_4$ was only partially converted to some paramagnetic species and PMe$_3$. This specific cobalt hydride complex was previously reported to catalyze the dimerization of phenylacetylene to enynes,[20] although the reaction conditions differed from ours. The dinuclear complex {(Me$_3$P)$_3$CoH}$_2$(N$_2$), which bears a more labile N$_2$ ligand, was reported to react with up to 4 equiv of phenylacetylene.[15] The isolated product was identified to be *mer,trans*-

https://doi.org/10.1021/acs.inorgchem.4c01993
Inorg. Chem. 2024, 63, 13689−13699

Scheme 1. C(sp)−H Bond Activation of Different Alkynes with $\{2,6\text{-}(^{i}Pr_2PO)_2C_6H_3\}Co(PMe_3)_2$[a]

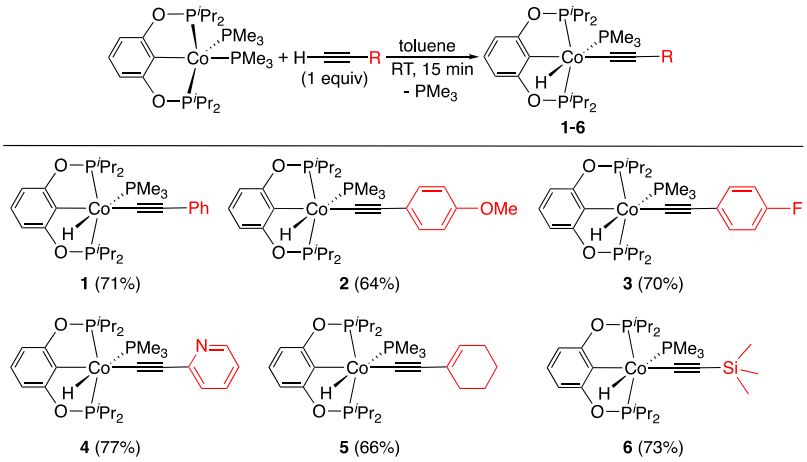

[a]Numbers in the parentheses are isolated yields.

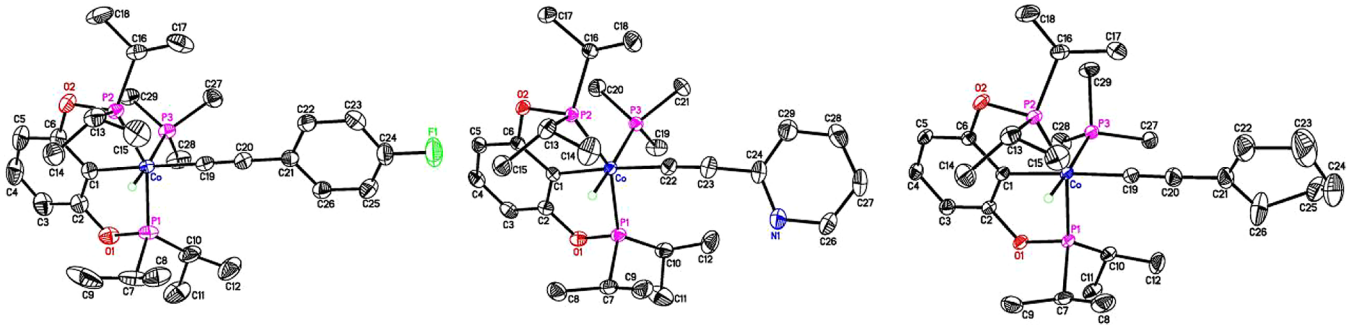

Figure 2. ORTEPs of $\{2,6\text{-}(^{i}Pr_2PO)_2C_6H_3\}CoH(C{\equiv}CC_6H_4F)(PMe_3)$ (**3**, left), $\{2,6\text{-}(^{i}Pr_2PO)_2C_6H_3\}CoH(C{\equiv}CC_5H_4N)(PMe_3)$ (**4**, middle), and $\{2,6\text{-}(^{i}Pr_2PO)_2C_6H_3\}CoH(C{\equiv}CC_6H_9)(PMe_3)$ (**5**, right) at the 50% probability level (all hydrogen atoms except the one bound to cobalt are omitted for clarity).

$\{(Me_3P)_3CoH(C{\equiv}CPh)_2$ (2 equiv), possibly resulting from a series of steps that eliminate N_2 and H_2. Our results here highlight the advantage of using a POCOP-type pincer ligand, which provides a robust platform for cobalt to perform oxidative addition reactions in a more straightforward fashion. The ancillary ligand PMe_3 is equally important for the reactions. Under the conditions similar to those outlined in eq 5, the dicarbonyl complex $\{2,6\text{-}(^{i}Pr_2PO)_2C_6H_3\}Co(CO)_2$ failed to react with phenylacetylene to yield any Co(III) hydride species.

To explore the generality of the C(sp)−H oxidative addition process, a diverse array of terminal alkynes was studied in reactions with $\{2,6\text{-}(^{i}Pr_2PO)_2C_6H_3\}Co(PMe_3)_2$. Introducing an electron-releasing or electron-withdrawing group (e.g., OMe or F) as the *para*-substituent on phenylacetylene had almost no impact on how the hydrido Co(III) alkynyl complex formed (Scheme 1). Replacing the phenyl group in phenylacetylene with a 2-pyridyl, 1-cyclohexenyl, or trimethylsilyl group also led to a fast and complete conversion of $\{2,6\text{-}(^{i}Pr_2PO)_2C_6H_3\}Co(PMe_3)_2$ to the corresponding C(sp)−H bond activated product. Like **1**, hydrido Co(III) alkynyl complexes **2**−**6** were readily isolated in modest yields (64−77%). These compounds were fully characterized by NMR and IR spectroscopy and elemental analyses. The solid-state structures of **3**−**5** were further studied by X-ray crystallography (Figure 2), confirming that the hydride ligand is consistently bound *trans* to PMe_3. Interestingly, **5** showed an off-white color in its solid form but gave a light blue solution when it was dissolved in C_6D_6. The freshly prepared **6** also appeared light in color but gradually turned to blue in weeks, even for a solid sample stored under an inert atmosphere. These observations hinted to us that **5** and **6** could be more inclined to undergo C(sp)−H reductive elimination because the resulting 4-coordinate cobalt complex, $\{2,6\text{-}(^{i}Pr_2PO)_2C_6H_3\}Co(PMe_3)$, is a dark blue compound.[3b] However, the NMR spectra of **5** and **6** (in C_6D_6) did not show resonances that could be definitively assigned to $\{2,6\text{-}(^{i}Pr_2PO)_2C_6H_3\}Co(PMe_3)$. It is possible that the quantity was below the NMR detection limit.

Alkyl-substituted acetylenes reacted with $\{2,6\text{-}(^{i}Pr_2PO)_2C_6H_3\}Co(PMe_3)_2$ differently. None of the stoichiometric reactions depicted in Scheme 2 could reach completion in 15 min. Evidently, the partial conversion was not due to kinetic reasons. Extending the reaction time for *tert*-butylacetylene or heating the reaction mixture to 80 °C actually *decreased* the ratio of $\{2,6\text{-}(^{i}Pr_2PO)_2C_6H_3\}CoH(C{\equiv}C^{t}Bu)(PMe_3)$ (**7**) to $\{2,6\text{-}(^{i}Pr_2PO)_2C_6H_3\}Co(PMe_3)_2$. This can be rationalized by cobalt-promoted oligomerization and/or polymerization of *tert*-butylacetylene that consumes the alkyne, thus shifting the equilibrium to the left side. The thermodynamic argument was further supported by mixing $\{2,6\text{-}(^{i}Pr_2PO)_2C_6H_3\}Co(PMe_3)_2$ with 20 equiv of *tert*-butylacetylene in C_6D_6, which resulted in full conversion of the starting Co(I) complex to **7** along with a minor decomposition product (~10%, δ_P = 51.2 ppm, consistent with $^{i}Pr_2P(=O)H$).[21] Various vinylic resonances were also observed in the ^1H NMR spectrum, presumably due to side

https://doi.org/10.1021/acs.inorgchem.4c01993
Inorg. Chem. 2024, 63, 13689−13699

Scheme 2. Terminal Alkynes in Equilibria with Their C(sp)−H Bond Activation Products[a]

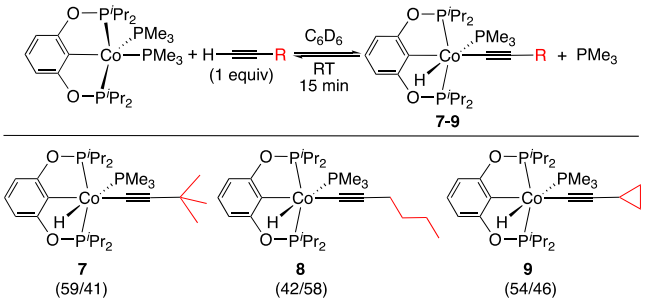

[a]Numbers in the parentheses are [CoH]/[Co(PMe$_3$)$_2$] ratios measured at the 15 min mark.

reactions of *tert*-butylacetylene. Unfortunately, attempts to isolate pure **7** were fruitless; the main challenge faced was the low stability of **7** under vacuum. The NMR spectra of the isolated product (a sticky substance) showed some unknown species and {2,6-(^{i}Pr$_2$PO)$_2$C$_6$H$_3$}Co(PMe$_3$), suggesting that reductive elimination of *tert*-butylacetylene had occurred. Our best method to obtain **7** as a solid started with dissolving {2,6-(^{i}Pr$_2$PO)$_2$C$_6$H$_3$}Co(PMe$_3$)$_2$ in neat *tert*-butylacetylene (bp = 37−38 °C), which afforded an almost colorless solution. An off-white precipitate slowly formed when the solution was kept at −30 °C. The solid was collected by decanting the supernatant liquid and analyzed as the desired hydrido Co(III) alkynyl complex, although it was contaminated with a decomposition product. 1-Hexyne and cyclopropylacetylene behaved similarly to *tert*-butylacetylene. Due to the purification challenges described above, the C(sp)−H oxidative addition products **7**−**9** were characterized only in solution by NMR spectroscopy.

The phosphorus chemical shift values of **1**−**9** are remarkably similar (Table 1), indicating that structural and electronic perturbations of the coordination sphere by the substituents on C≡C are negligible. The substituent effects on the hydride chemical shift values are also small, although the Co(III) hydride complexes originating from alkyl-substituted acetylenes (i.e., **7**−**9**) all have more negative values. The bond lengths determined by X-ray crystallography confirm that there are very little structural variations in the Co−C$_{alkyne}$, C≡C, and Co−H bonds, at least among **1** and **3**−**5**.[22]

The distinct reactivities displayed by the alkynes in Schemes 1 and 2 may reflect the differences in Co−C$_{alkyne}$ bond strengths, which are not always inferable from the NMR and crystallographic data.[23] Our previous study of {2,6-(^{i}Pr$_2$PO)$_2$C$_6$H$_3$}NiSAr (Ar = *para*-substituted phenyl group) revealed that introducing an electron-withdrawing substituent makes the Ni−S bond stronger.[24] The substituent effects on the S−H bond dissociation energies of ArSH follow a similar trend, although the effects are smaller. We attributed this phenomenon to the increased electrostatic contribution to the Ni−S bonding. The alkyne substrates listed in Scheme 1 either contain a sp^2-hybridized carbon directly attached to the C≡C bond or, in the case of trimethylsilylacetylene, involve hyperconjugative interactions between the low-lying Si−C σ^* orbitals and the alkyne π orbitals.[25] Considering that Co(III) is a hard acid, the aryl, alkenyl, and silyl groups (as harder bases) likely strengthen the Co−C$_{alkyne}$ bonds and improve the thermodynamics of the C(sp)−H oxidative addition process. The reactivity does not appear to correlate with the C−H acidity. Nitromethane (p$K_{a\ (DMSO)}$ = 17.2), malononitrile (p$K_{a\ (DMSO)}$ = 11.1), and diethyl malonate (p$K_{a\ (DMSO)}$ = 16.4), which are significantly more acidic than phenylacetylene (p$K_{a\ (DMSO)}$ = 28.8), failed to react with {2,6-(^{i}Pr$_2$PO)$_2$C$_6$H$_3$}-Co(PMe$_3$)$_2$ (eq 6). Similarly, pentafluorobenzene did not undergo C(sp^2)−H oxidative addition with the Co(I) pincer complex. To eliminate the potential complications caused by the dissociated PMe$_3$, the hydrido Co(III) alkynyl complex **2** was also treated with diethyl malonate and pentafluorobenzene; neither case produced a new hydride species.

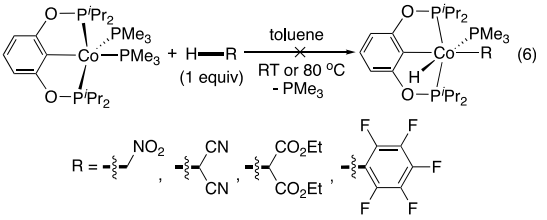

S−H Oxidative Addition. Oxidative addition of thiols to a low-valent metal species has been implicated in catalytic hydrothiolation of carbon−carbon multiple bonds.[26] Well-defined metal systems that can perform this type of reaction are actually scarce. Most of the known examples involve second or third row transition metals,[27] heterobimetallic compounds,[28] or clusters.[29] As far as cobalt-based systems are concerned, trimethylphosphine-ligated complexes including (Me$_3$P)$_3$CoCl,[30] (Me$_3$P)$_4$Co,[30] (Me$_3$P)$_4$CoMe,[30,31] and even the high-valent (Me$_3$P)$_3$CoMe$_3$[32] have been used to activate thiols, although the mechanistic information about S−H oxidative addition is lost in the complexity of the reactions (e.g., consecutive S−H bond activation and/or an elimination step involving the SH hydrogen). A tridentate *N*-heterocyclic phosphido Co(I) complex has also been reported to activate PhSH; however, the thiol is added across the Co−P bond without changing the metal oxidation state.[33] The POCOP-

Table 1. Key NMR and Crystallographic Data of {2,6-(^{i}Pr$_2$PO)$_2$C$_6$H$_3$}CoH(C≡CR)(PMe$_3$)

R group	δ_P (in C$_6$D$_6$)	δ_{CoH} (in C$_6$D$_6$)	Co−C$_{alkyne}$ (Å)	C≡C (Å)	Co−H (Å)
phenyl (**1**)	205.8, −1.9	−12.76	1.9034(13)	1.2154(19)	1.401(18)
4-methoxyphenyl (**2**)	205.6, −1.8	−12.75			
4-fluorophenyl (**3**)	205.6, −1.8	−12.80	1.909(2)	1.217(3)	1.373(24)
2-pyridyl (**4**)	206.2, −2.0	−12.74	1.8985(13)	1.2150(19)	1.400(18)
1-cyclohexenyl (**5**)	205.3, −2.0	−12.80	1.914(2)	1.221(4)	1.281(27)
trimethylsilyl (**6**)	205.2, −3.4	−12.77			
tert-butyl (**7**)	205.1, −2.3	−12.88			
n-butyl (**8**)	205.2, −2.0	−12.86			
cyclopropyl (**9**)	205.0, −2.1	−12.90			

https://doi.org/10.1021/acs.inorgchem.4c01993
Inorg. Chem. 2024, 63, 13689−13699

type pincer system reported here provides a definitive example of S−H oxidative addition that takes place at a Co(I) center.

First, NMR experiments were conducted by mixing {2,6-(^{i}Pr$_2$PO)$_2$C$_6$H$_3$}Co(PMe$_3$)$_2$ with PhSH (1−5 equiv) in C$_6$D$_6$, which rapidly formed the free PMe$_3$ and a hydride species with a diagnostic resonance at −12.07 ppm (a doublet of triplets, $^2J_{H-P}$ = 100.4 and 68.0 Hz). In addition to these expected products, 1,3-(^{i}Pr$_2$PO)$_2$C$_6$H$_4$ and ^{i}Pr$_2$P(=O)H were also observed as minor impurities. The formation of the diphosphinite is informative, suggesting that C(sp^2)−H reductive elimination can occur with the hydrido Co(III) thiolate complex. Mixing 1,3-(^{i}Pr$_2$PO)$_2$C$_6$H$_4$ with 5 equiv PhSH in C$_6$D$_6$ showed degradation of the diphosphinite but at a rate significantly slower than those of S−H oxidation addition and C(sp^2)−H reductive elimination. In other words, pincer degradation must take place when the ligand is still bound to the metal. To fully characterize the oxidative addition product, a preparative scale reaction was performed (eq 7), which led to the isolation of {2,6-(^{i}Pr$_2$PO)$_2$C$_6$H$_3$}CoH(SPh)(PMe$_3$) (**10**) as an orange solid. The structure of this complex, particularly the position of the SPh group relative to the ipso carbon, was unambiguously established by X-ray crystallography (Figure 3). Compared to the structures of **1** and **3**−**5**, the three Co−P bonds in **10** are elongated by 0.02−0.03 Å. These structural variations are in agreement with the phosphorus resonances of **10** (197.2 and −7.4 ppm), which are upfield-shifted from those of the hydrido Co(III) alkynyl complexes (Table 1), although the electronic effects (SPh vs C≡CR) on the phosphorus chemical shift values may also be important.

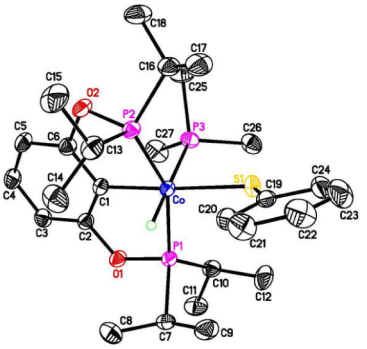

Figure 3. ORTEP of {2,6-(^{i}Pr$_2$PO)$_2$C$_6$H$_3$}CoH(SPh)(PMe$_3$) (**10**) at the 50% probability level (all hydrogen atoms except the one bound to cobalt are omitted for clarity). Selected bond lengths (Å) and angles (deg): Co−C1 1.9269(15), Co−S1 2.2940(5), Co−P1 2.1722(4), Co−P2 2.1802(4), Co−P3 2.2677(4), Co−H 1.440(21); P1−Co−P2 154.220(18), C1−Co−P3 86.99(5), C1−Co−S1 175.87(5).

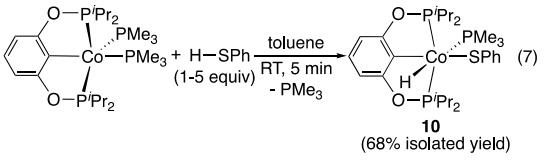

The solid sample of **10** was shown to be stable under an inert atmosphere. In contrast, **10** in solution (in C$_6$D$_6$ sealed in a J. Young NMR tube) turned darker over time even without heating. The NMR spectra recorded after 3 days showed that ∼25% of **10** was converted to 1,3-(^{i}Pr$_2$PO)$_2$C$_6$H$_4$ along with some paramagnetic species. Replacing the alkynyl groups in **1** and **3**−**5** with the SPh group only makes the C$_{ipso}$−Co bond marginally shorter (by 0.01 Å or less). Nevertheless, the effect can be augmented by the elongation of the Co−P bonds that may lower the kinetic barrier for C(sp^2)−H reductive elimination as well as the dissociation of 1,3-(^{i}Pr$_2$PO)$_2$C$_6$H$_4$ from cobalt.

As a representative example for aliphatic thiols, 1-pentanethiol was selected to react with {2,6-(^{i}Pr$_2$PO)$_2$C$_6$H$_3$}-Co(PMe$_3$)$_2$ in C$_6$D$_6$ (eq 8). The reaction yielded the expected product {2,6-(^{i}Pr$_2$PO)$_2$C$_6$H$_3$}CoH(SC$_5$H$_{11}$)(PMe$_3$) (**11**), signaled by a hydride resonance at −12.74 ppm and two phosphorus resonances at 196.3 and −5.3 ppm. However, the S−H oxidative addition did not reach completion (∼85% conversion) even when 5 equiv of 1-pentanethiol was added and the reaction time was extended to 24 h. An extensive degradation of the pincer ligand and the formation of 1,3-(^{i}Pr$_2$PO)$_2$C$_6$H$_4$ were also observed. Studies of POCOP-type nickel pincer complexes have already taught us that the O−P bonds are susceptible to attack by a nucleophile to trigger decomposition pathways.[34] It is thus not surprising that the reaction of 1-pentanethiol with {2,6-(^{i}Pr$_2$PO)$_2$C$_6$H$_3$}Co-(PMe$_3$)$_2$ is less selective. The coexistence of both starting materials with **11** does suggest that they are in equilibrium. Similar to C(sp)−H bond activation with alkynes, the S−H oxidative addition process becomes less favorable when the thiol substituent switches from an aryl group to an alkyl group.

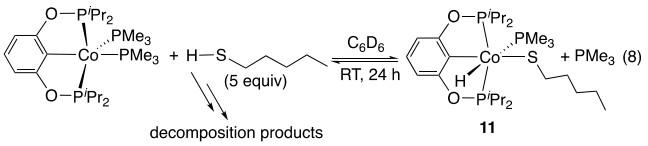

Sn−H Oxidative Addition. Both C(sp)−H and S−H bonds are polarized in such a way that the hydrogen atom carries a slight positive charge. The polarization is reversed with Sn−H bonds due to the comparatively low electronegativity associated with tin. In light of this, we wished to know if the Co(I) pincer complex could also cleave Sn−H bonds following an oxidative addition pathway. This type of reaction has been less frequently explored in the past.[35] To the best of our knowledge, the only relevant work with a cobalt complex involves the reactions of in situ generated "(triphos)-Co" (triphos = CH$_3$C(CH$_2$PPh$_2$)$_3$) with Ph$_3$SnH and ^{n}Bu$_3$SnH to give (triphos)CoSnPh$_3$ and (triphos)-CoH$_2$(Sn^{n}Bu$_3$), respectively.[36]

To test the reactivity of organotin hydrides, Ph$_3$SnH (1 equiv) was first added to the solution of {2,6-(^{i}Pr$_2$PO)$_2$C$_6$H$_3$}-Co(PMe$_3$)$_2$ in C$_6$D$_6$, which resulted in a rapid color change from dark red to light yellow. The NMR spectra confirmed that the reaction was selective, producing a 1:1 mixture of PMe$_3$ and {2,6-(^{i}Pr$_2$PO)$_2$C$_6$H$_3$}CoH(SnPh$_3$)(PMe$_3$) (**12**). The hydride resonance of **12** was found at −15.59 ppm, which is shifted significantly from those of **1**−**11** (i.e., from −12.07 to −12.90 ppm). Apart from the tin satellites ($^2J_{H-Sn}{}^{117,119}$ = 276 Hz), the splitting pattern for the hydride remains a doublet of triplets; however, the *trans* ^{1}H−Co−^{31}P coupling constant in **12** is noticeably smaller (81.2 Hz vs 100.8−111.6 Hz in **1**−**11**). The phosphorus resonances for the pincer ligand and PMe$_3$ were located at 209.6 and −6.3 ppm, respectively. The former is shifted downfield relative to the phosphinite ^{31}P resonances in **1**−**11**. By and large, the NMR data indicate that the introduction of the SnPh$_3$ group onto the

https://doi.org/10.1021/acs.inorgchem.4c01993
Inorg. Chem. 2024, 63, 13689−13699

cobalt brings a substantial change to the molecular geometry and the electronic environment around the metal.

For a more complete characterization of the oxidative addition product, **12** was isolated (as a yellow solid) from a reaction carried out in benzene (eq 9) and studied spectroscopically. The presence of a Co−H bond was confirmed by an IR band at 1951 cm^{-1}, albeit with low intensity. The success of forming a cobalt stannyl complex was supported by a broad ^{119}Sn resonance at −35.0 ppm (in C_6D_6), which is comparable to the ^{119}Sn resonance of (triphos)Co(CO)$SnPh_3$ (−31.4 ppm).[36] Single crystals suitable for crystallographic studies were obtained from a reaction of {2,6-(^{i}Pr$_2$PO)$_2$C$_6$H$_3$}Co(PMe$_3$)$_2$ with Ph_3SnH performed in pentane. As shown in Figure 4, the hydride

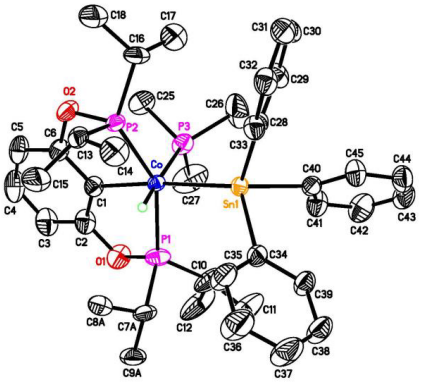

Figure 4. ORTEP of {2,6-(^{i}Pr$_2$PO)$_2$C$_6$H$_3$}CoH(SnPh$_3$)(PMe$_3$) (**12**) at the 50% probability level (all hydrogen atoms except the one bound to cobalt are omitted for clarity). Selected bond lengths (Å) and angles (deg): Co−C1 1.963(4), Co−Sn1 2.5598(5), Co−P1 2.1717(11), Co−P2 2.1840(10), Co−P3 2.2576(11), Co−H 1.329(57); P1−Co−P2 148.70(5), C1−Co−P3 86.57(12), C1−Co−Sn1 174.11(12).

ligand is again *trans* to PMe_3, leaving the $SnPh_3$ group *trans* to the ipso carbon. Structural comparison of **12** with **1** and **3**−**5** suggests that the three Co−P bonds are elongated by ∼0.02 Å, probably to accommodate the bulky $SnPh_3$ group. These bond lengths are, however, very similar to those in thiolate complex **10**. What sets **12** apart from **10** is a longer Co−C_{ipso} bond [1.963(4) Å in **12** vs 1.9269(15) Å in **10**] and a smaller ^{i}Pr$_2$P−Co−P^{i}Pr$_2$ angle (148.70(5)° in **12** vs 154.220(18)° in **10**). Despite the lack of conformational flexibility with the POCOP-type pincer ligands,[37] the Co−C_{ipso} bond can serve as a reporter for the *trans*-influence of the opposing ligand. The crystallographic data of **1**, **3**−**5**, **10**, **12**, and the previously reported {2,6-(^{i}Pr$_2$PO)$_2$C$_6$H$_3$}CoH(SiH$_2$Ph)(PMe$_3$)[3b] allow us to deduce a *trans*-influence series of $SnPh_3$ ∼ SiH_2Ph > C≡CR > SPh, which agrees reasonably well with the order calculated for *trans*-(Me$_3$P)$_2$PtX(Cl).[38]

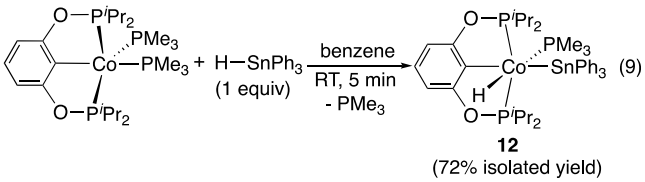

As one might have anticipated, replacing Ph_3SnH with ^{n}Bu$_3$SnH resulted in an incomplete reaction with {2,6-(^{i}Pr$_2$PO)$_2$C$_6$H$_3$}Co(PMe$_3$)$_2$. When ^{n}Bu$_3$SnH was added in large excess (10 equiv), ∼95% of the Co(I) pincer complex was converted to {2,6-(^{i}Pr$_2$PO)$_2$C$_6$H$_3$}CoH(Sn^{n}Bu$_3$)(PMe$_3$) (**13**) along with the dissociated PMe_3 (eq 10). Attempts to purify **13** were thwarted by the reversibility of the reaction and the decomposition of the product during workup. The oxidative addition product generated in situ (in C_6D_6) displayed a hydride resonance at −15.82 ppm as a doublet of triplets ($^2J_{H-P}$ = 78.8 and 68.8 Hz) with tin satellites ($^2J_{H-Sn}^{117,119}$ = 272 Hz) and two phosphorus resonances at 212.0 and −2.8 ppm. The presence of a Co−Sn^{n}Bu$_3$ moiety was confirmed by a broad ^{119}Sn resonance centered at 5.7 ppm; for comparison, (triphos)Co(H)$_2$(Sn^{n}Bu$_3$) was reported to have a ^{119}Sn resonance at 17.8 ppm.[36]

Table 2. Hydrostannation of Alkynes with Ph_3SnH[a]

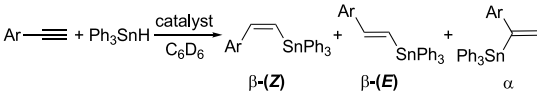

entry	Ar	catalyst (catalyst loading)	temperature, time	conversion	β-(Z):β-(E):α
1[b]	4-CH$_3$OC$_6$H$_4$	(L$_2$X)Co(PMe$_3$)$_2$ (5 mol %)	RT, 12 h	>99%	95:4:1
2[c]	4-CH$_3$OC$_6$H$_4$	(L$_2$X)Co(PMe$_3$)$_2$ (5 mol %)	RT, 12 h	>99%	91:6:3
3	4-CH$_3$OC$_6$H$_4$	(L$_2$X)Co(PMe$_3$)$_2$ (5 mol %)	80 °C, 2 h	>99%	54:35:11
4	4-CH$_3$OC$_6$H$_4$	(L$_2$X)Co(PMe$_3$)$_2$ (0.5 mol %)	RT, 24 h	91%	48:34:18
5	4-CH$_3$OC$_6$H$_4$	**12** (5 mol %)	RT, 12 h	83%	49:38:13
6	4-CH$_3$OC$_6$H$_4$	**2** (5 mol %)	RT, 12 h	82%	50:37:13
7	4-CH$_3$OC$_6$H$_4$	no catalyst	RT, 24 h	40%	66:33:1
8	4-CH$_3$OC$_6$H$_4$	no catalyst	RT, 24 h then 80 °C, 2 h	82%	26:73:1
9	4-CH$_3$OC$_6$H$_4$	PMe$_3$ (5 mol %)	RT, 24 h	13%	87:13:<1
10	4-CH$_3$OC$_6$H$_4$	PMe$_3$ (5 mol %)	RT, 24 h then 80 °C, 2 h	80%	30:68:2
11	4-FC$_6$H$_4$	(L$_2$X)Co(PMe$_3$)$_2$ (5 mol %)	RT, 12 h	>99%	95:5:<1
12	C$_6$H$_5$	(L$_2$X)Co(PMe$_3$)$_2$ (5 mol %)	RT, 12 h	97%	>99:<1:<1

[a]Reaction conditions: ArC≡CH (0.18 mmol), Ph_3SnH (0.22 mmol), and a catalyst mixed in C_6D_6 (600 μL) and kept in the dark. Conversions and product ratios were determined by NMR spectroscopy. [b](L$_2$X)Co(PMe$_3$)$_2$ = {2,6-(^{i}Pr$_2$PO)$_2$C$_6$H$_3$}Co(PMe$_3$)$_2$. RT = 23 °C. [c]Reaction was exposed to ambient fluorescent light.

https://doi.org/10.1021/acs.inorgchem.4c01993
Inorg. Chem. 2024, 63, 13689−13699

Scheme 3. Hydrostannation of 4-Ethynylanisole with Ph_3SnH Following a "Tin Hydride-First" or an "Alkyne-First" Approach

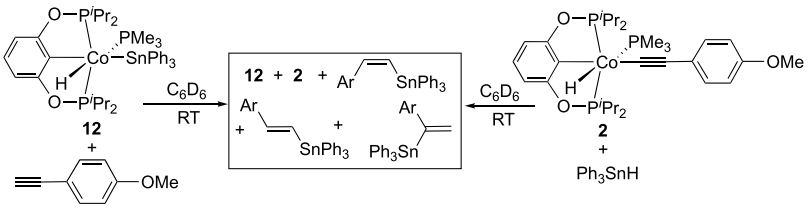

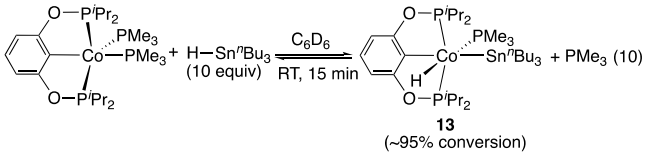

Implications in Catalysis. The fact that {2,6-(^{i}Pr$_2$PO)$_2$C$_6$H$_3$}Co(PMe$_3$)$_2$ can activate both terminal alkynes and thiols prompted us to explore its catalytic activity for the hydrothiolation of terminal alkynes. In our first attempted catalytic study, PhSH, phenylacetylene, and {2,6-(^{i}Pr$_2$PO)$_2$C$_6$H$_3$}Co(PMe$_3$)$_2$ were mixed in a 24:20:1 ratio (in C_6D_6) and monitored by NMR spectroscopy. No hydrothiolation products were detected when the mixture was kept at room temperature or heated at 80 °C for 16 h. Similarly, compound **1** isolated from the C(sp)–H oxidative addition reaction (eq 5) showed no catalytic activity for the hydrothiolation of phenylacetylene with PhSH. In fact, mixing **1** with PhSH (1 or 2 equiv) resulted in rapid formation of the S–H bond activated product **10** and phenylacetylene (eq 11). According to the commonly proposed mechanisms for the hydrothiolation reaction,[26a] **1** could potentially undergo isomerization to give a vinylidene intermediate, which in turn could be subject to a nucleophilic attack by the thiol. Alternatively, **10** could dissociate PMe_3 to allow the alkyne to bind to cobalt and then insert into the Co–SR bond. The lack of catalytic reactivity here suggests that neither process is feasible with the POCOP-pincer supported cobalt system.

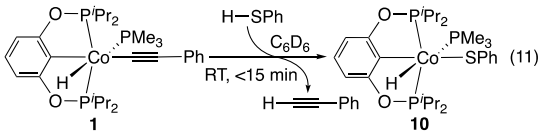

Catalytic hydrostannation of alkynes provides quick access to alkenylstannanes that can be used for Kosugi-Migita-Stille cross-coupling reactions.[39] To date, many transition metal-based catalysts have been developed, although for cobalt-based systems, only $CoCl_2(PPh_3)_2$ is known to catalyze the hydrostannation of alkynes and the results were not always reproducible.[40] This motivated us to conduct a series of experiments focusing on the reaction of 4-ethynylanisole with Ph_3SnH catalyzed by the cobalt pincer complexes.[41] When {2,6-(^{i}Pr$_2$PO)$_2$C$_6$H$_3$}Co(PMe$_3$)$_2$ was employed as the catalyst (5 mol %), the reaction studied at room temperature was complete within 12 h, affording a 95:4:1 mixture favoring the β-(Z) isomer (Table 2, entry 1). The catalytic reaction was performed in the dark to minimize the degradation of Ph_3SnH to Ph_6Sn_2.[42] However, a sample intentionally exposed to ambient light throughout the experiment showed very similar results in terms of both conversion and regioselectivity (entry 2). Raising the temperature to 80 °C (entry 3) or lowering the catalyst loading to 0.5 mol % (entry 4) led to a significant erosion of regioselectivity and, notably, an increased amount of the α isomer. To our surprise, the Co(III) hydride complexes **12** and **2** resulting from Sn–H and C(sp)–H bond activation, respectively, displayed diminished catalytic activity when compared to the parent complex, {2,6-(^{i}Pr$_2$PO)$_2$C$_6$H$_3$}Co(PMe$_3$)$_2$ (entries 5 and 6 vs entry 1). In addition, the regioselectivity was poorer when the reaction was catalyzed by **12** or **2**, with the β-(Z) isomer representing only ~50% of the total hydrostannation products.

Hydrostannation of alkynes can take place without a catalyst but often requires heating.[43] Our control experiment confirmed that, at room temperature for 24 h, the uncatalyzed reaction converted 40% of 4-ethynylanisole to a 66:33:1 mixture of the β-(Z), β-(E), and α isomers (Table 2, entry 7). Heating this reaction mixture at 80 °C for an additional 2 h increased the conversion of 4-ethynylanisole to 82% and the percentage of the thermodynamically more stable β-(E) isomer to 73% (entry 8). Considering that PMe_3 can be released from {2,6-(^{i}Pr$_2$PO)$_2$C$_6$H$_3$}Co(PMe$_3$)$_2$, we also ran a control experiment of the hydrostannation reaction in the presence of PMe_3 (5 mol %). Interestingly, PMe_3 played an inhibitory role when the reaction was carried out at room temperature (entry 9 vs entry 7), although at 80 °C, the effect was negligible (entry 10 vs entry 8). It is possible that PMe_3 may interact with the tin hydride[44] or perhaps intercept some radical intermediates[45] that could slow down the hydrostannation process.

At this point, the mechanistic details for the cobalt-catalyzed hydrostannation of 4-ethynylanisole with Ph_3SnH remain unclear to us. The reaction is unlikely catalyzed by nonpincer fragments because, under the catalytic conditions, degradation of the pincer framework is negligible. What is more certain is that {2,6-(^{i}Pr$_2$PO)$_2$C$_6$H$_3$}Co(PMe$_3$)$_2$ and **12**/**2** follow different mechanistic pathways, as judged by the discrepancy in conversion and regioselectivity (Table 2, entries 5 and 6 vs entry 1). The two Co(III) hydride complexes nonetheless converge to the same catalytic cycle. The stoichiometric reaction of **12** with 4-ethynylanisole and the stoichiometric reaction of **2** with Ph_3SnH were studied separately (Scheme 3). The two experiments yielded a nearly identical mixture that consisted of **12**, **2**, and the three hydrostannation products with isomeric ratios similar to those observed in the catalytic reactions. Studies of other metal systems have suggested that alkyne insertion into a M–Sn bond favors the α isomers.[46] Such a mechanism could be operating here, especially with **12** (or **2** via **12**), but is unlikely to be the major pathway. Using {2,6-(^{i}Pr$_2$PO)$_2$C$_6$H$_3$}Co(PMe$_3$)$_2$ as the catalyst undoubtedly changes the reaction mechanism so that the selectivity favors the β-(Z) isomer, not only for 4-ethynylanisole but also for 1-ethynyl-4-fluorobenzene and phenylacetylene (Table 2, entries 11 and 12). We speculate that a Lewis acidic cobalt center and the dissociated PMe_3 might act synergistically in catalyzing the reaction. This hypothesis will be tested experimentally and computationally in a future study.

https://doi.org/10.1021/acs.inorgchem.4c01993
Inorg. Chem. 2024, 63, 13689–13699

CONCLUSIONS

In summary, we have demonstrated that the combination of a POCOP-type pincer ligand and PMe_3 allows Co(I) to activate C(sp)−H, S−H, and Sn−H bonds via an oxidative addition pathway. These reactions are reversible, implying that reductive elimination reactions with the Co(III) species are also feasible on the same ligand platform. The equilibria are greatly influenced by the substituents on acetylenes, thiols, and tin hydrides; it can be generalized that having electron-withdrawing substituents favors the oxidative addition products. The formation of the hydrido Co(III) alkynyl, thiolate, and stannyl complexes could provide the must-needed mechanistic basis for transition metal-catalyzed hydrothiolation and hydrostannation of alkynes. On the other hand, our failed hydrothiolation reaction comes as a warning that the success of a metal complex to activate both reactants does not necessarily translate to a successful catalytic reaction. In any case, our Co(I) pincer complex is an effective catalyst for the hydrostannation of terminal alkynes with Ph_3SnH that can yield β-(*E*)-alkenylstannanes selectively. Despite the fact that the alkynes and Ph_3SnH can be added oxidatively to Co(I), the resulting hydrido Co(III) alkynyl and stannyl complexes are unlikely involved as the main intermediates in the catalytic cycles. Our future efforts will be focused on further mechanistic elucidation and the reactions of molecules with more polarized bonds.

EXPERIMENTAL SECTION

General Methods. Unless otherwise noted, all organometallic compounds were prepared and handled under an argon atmosphere using standard glovebox and Schlenk techniques. Dry and oxygen-free toluene and pentane were collected from an Innovative Technology solvent purification system and used throughout the experiments. Benzene-d_6 (99.5% D) and benzene were dried over sodium benzophenone and distilled under an argon atmosphere. Anhydrous and inhibitor-free tetrahydrofuran (THF) was purchased from Sigma-Aldrich (packed in a Sure/Seal bottle) and used as received without further purification. $\{2,6\text{-}(^iPr_2PO)_2C_6H_3\}Co(PMe_3)_2$,[3b] $HCo(PMe_3)_4$,[47] and $\{2,6\text{-}(^iPr_2PO)_2C_6H_3\}Co(CO)_2$[3a] were prepared as described in the literature. Triphenyltin hydride (95%) was purchased from AA Blocks, and *tert*-butylacetylene (98%) was purchased from Thermo Scientific Chemicals; they were used as received without further purification. NMR spectra were recorded on a Bruker AV400 or NEO400 NMR spectrometer. The chemical shift values for ^1H and $^{13}C\{^1H\}$ NMR spectra were referenced internally to the residual solvent resonances. $^{31}P\{^1H\}$ spectra were referenced externally to 85% H_3PO_4 (0 ppm). $^{119}Sn\{^1H\}$ NMR spectra were referenced externally to $SnMe_4$ in a 5% v/v solution (0 ppm, in C_6D_6). Using this reference, the ^{119}Sn resonances of Ph_3SnH and Ph_6Sn_2 (present in the purchased sample of Ph_3SnH) appeared at −161.4 and −139.8 ppm, respectively. IR spectra were recorded on a PerkinElmer Spectrum Two Fourier transform infrared spectrometer equipped with a Smart Orbit diamond attenuated-total-reflectance (ATR) accessory. Synthetic procedures and characterization data for the representative compounds (**1**, **10**, and **12**) are described below. The results for other cobalt complexes are provided in the Supporting Information.

Safety Statement. Most organotin compounds are highly toxic and should be carefully handled in a well-ventilated fume hood while wearing appropriate PPE.

Synthesis of $\{2,6\text{-}(^iPr_2PO)_2C_6H_3\}CoH(C{\equiv}CPh)(PMe_3)$ (1). In a flame-dried Schlenk flask, $\{2,6\text{-}(^iPr_2PO)_2C_6H_3\}Co(PMe_3)_2$ (50 mg, 0.091 mmol) was dissolved in ∼10 mL of toluene, after which phenylacetylene (10.0 μL, 0.091 mmol) was added. The resulting mixture was stirred at room temperature for 15 min and then filtered into another Schlenk flask (via a cannula) to remove a small amount of insoluble material. Evaporating the toluene solution under vacuum afforded the desired product as an off-white solid (37 mg, 71% yield). X-ray quality crystals were grown at room temperature in a scintillation vial by slow diffusion of pentane into a saturated solution of **1** in toluene. ^1H NMR (400 MHz, C_6D_6, δ): 7.42 (d, $^3J_{H-H}$ = 8.0 Hz, Ar*H*, 2H), 7.15−7.12 (m, Ar*H*, 2H), 6.95 (t, $^3J_{H-H}$ = 8.0 Hz, Ar*H*, 1H), 6.80 (t, $^3J_{H-H}$ = 8.0 Hz, Ar*H*, 1H), 6.63 (d, $^3J_{H-H}$ = 7.6 Hz, Ar*H*, 2H), 2.79−2.64 (m, C*H*$(CH_3)_2$, 2H), 2.61−2.44 (m, C*H*$(CH_3)_2$, 2H), 1.67−1.52 (m, CH(C*H*$_3)_2$, 6H), 1.47−1.37 (m, CH(C*H*$_3)_2$, 6H), 1.37−1.27 (m, CH(C*H*$_3)_2$, 6H), 1.13−1.03 (m, CH(C*H*$_3)_2$, 6H), 0.99 (d, $^2J_{H-P}$ = 7.2 Hz, P(C*H*$_3)_3$, 9H),−12.76 (dt, $^2J_{H-P}$ = 111.6 and 60.8 Hz, Co*H*, 1H). $^{13}C\{^1H\}$ NMR (101 MHz, C_6D_6, δ): 164.4 (td, *J* = 9.1 and 4.0 Hz, C_2 and C_6 of the pincer unit), 131.2 (s, Ar*C*), 130.6 (s, Ar*C*), 127.4 (s, Ar*C*), 125.7 (d, $^3J_{C-P}$ = 3.0 Hz, Co*C* ≡ *C*), 123.8 (s, Ar*C*), 116.8 (s, Ar*C*), 104.6 (td, *J* = 5.0 and 3.2 Hz, C_3 and C_5 of the pincer unit), 34.9 (td, *J* = 8.8 and 4.1 Hz, *C*H$(CH_3)_2$), 30.1 (td, *J* = 13.8 and 10.0 Hz, *C*H$(CH_3)_2$), 18.5 (dt, $^1J_{C-P}$ = 9.3 Hz, $^3J_{C-P}$ = 4.2 Hz, P$(CH_3)_3$), 18.1 (t, *J* = 2.0 Hz, CH(*C*H$_3)_2$), 18.0 (s, CH(*C*H$_3)_2$), 17.9 (t, *J* = 2.0 Hz, CH(*C*H$_3)_2$), 17.1 (t, *J* = 2.2 Hz, CH(*C*H$_3)_2$); the two Co*C* resonances were not located. $^{31}P\{^1H\}$ NMR (162 MHz, C_6D_6, δ): 205.8 (br, O*P*^{i}Pr$_2$, 2P),−1.9 (br, *P*Me$_3$, 1P). Selected ATR-IR data (solid, cm^{-1}): 2087 ($\nu_{C\equiv C}$), 1977 (ν_{Co-H}). Anal. Calcd for $C_{29}H_{46}O_2P_3Co$: C, 60.21; H, 8.01. Found: C, 60.32; H, 8.02.

Synthesis of $\{2,6\text{-}(^iPr_2PO)_2C_6H_3\}CoH(SPh)(PMe_3)$ (10). To a flame-dried Schlenk flask equipped with a stir bar were added $\{2,6\text{-}(^iPr_2PO)_2C_6H_3\}Co(PMe_3)_2$ (25 mg, 0.045 mmol), toluene (∼10 mL), and thiophenol (9.3 μL, 0.091 mmol). The mixture was stirred at room temperature for 5 min and then concentrated under vacuum. The resulting yellowish oily residue was treated with pentane (5 mL × 3) and filtered into another Schlenk flask via a cannula. The combined pentane solutions were concentrated under vacuum to ∼1 mL and kept in a−30 °C freezer. Crystals formed within a day, which were collected by decanting the mother liquor and dried under vacuum. The desired product was isolated as an orange solid (18 mg, 68% yield). X-ray quality crystals were grown at −30 °C in a scintillation vial from a saturation solution of **10** in pentane. ^1H NMR (400 MHz, C_6D_6, δ): 7.95 (d, $^3J_{H-H}$ = 6.8 Hz, Ar*H*, 2H), 7.10 (t, $^3J_{H-H}$ = 7.6 Hz, Ar*H*, 2H), 6.89 (t, $^3J_{H-H}$ = 6.8 Hz, Ar*H*, 1H), 6.75 (t, $^3J_{H-H}$ = 8.0 Hz, Ar*H*, 1H), 6.56 (d, $^3J_{H-H}$ = 8.0 Hz, Ar*H*, 2H), 2.90 (heptet of virtual triplets, $^3J_{H-H}$ = 7.2 Hz, *J* = 2.3 Hz, C*H*$(CH_3)_2$, 2H), 2.45 (heptet, $^3J_{H-H}$ = 7.2 Hz, C*H*$(CH_3)_2$, 2H), 1.40−1.24 (m, CH(C*H*$_3)_2$, 18H), 1.24−1.17 (m, CH(C*H*$_3)_2$, 6H), 0.90 (d, $^2J_{H-P}$ = 7.2 Hz, P(C*H*$_3)_3$, 9H),−12.07 (dt, $^2J_{H-P}$ = 100.4 and 68.0 Hz, Co*H*, 1H). $^{13}C\{^1H\}$ NMR (101 MHz, C_6D_6, δ): 164.9 (td, *J* = 8.9 and 4.6 Hz, C_2 and C_6 of the pincer unit), 150.4 (d, $^3J_{C-P}$ = 13.1 Hz, CoSC), 135.2 (s, Co*C*), 132.4 (s, Ar*C*), 127.3 (s, Ar*C*), 125.9 (d, $^4J_{C-P}$ = 3.7 Hz, C_2 and C_6 of the SPh group), 120.8 (s, Ar*C*), 104.9 (td, *J* = 5.1 and 3.9 Hz, C_3 and C_5 of the pincer unit), 34.7 (td, *J* = 7.4 and 4.7 Hz, *C*H$(CH_3)_2$), 32.4 (td, *J* = 13.0 and 9.6 Hz, *C*H$(CH_3)_2$), 18.9 (t, *J* = 2.5 Hz, CH(*C*H$_3)_2$), 18.5 (s, CH(*C*H$_3)_2$), 17.8 (s, CH(*C*H$_3)_2$), 17.6 (t, *J* = 2.3 Hz, CH(*C*H$_3)_2$), 16.2 (dt, $^1J_{C-P}$ = 21.4 Hz, $^3J_{C-P}$ = 1.8 Hz, P(*C*H$_3)_3$). $^{31}P\{^1H\}$ NMR (162 MHz, C_6D_6, δ): 197.2 (br, O*P*^{i}Pr$_2$, 2P),−7.4 (br, *P*Me$_3$, 1P). Selected ATR-IR data (solid, cm^{-1}): 1959 (ν_{Co-H}). Anal. Calcd for $C_{27}H_{46}O_2P_3SCo$: C, 55.29; H, 7.90. Found: C, 55.43; H, 8.02.

Synthesis of $\{2,6\text{-}(^iPr_2PO)_2C_6H_3\}CoH(SnPh_3)(PMe_3)$ (12). In a flame-dried Schlenk flask, $\{2,6\text{-}(^iPr_2PO)_2C_6H_3\}Co(PMe_3)_2$ (50 mg, 0.091 mmol) was dissolved in ∼10 mL of benzene, after which triphenyltin hydride (32 mg, 0.091 mmol) was added. The resulting mixture was stirred at room temperature for 5 min and then filtered into another Schlenk flask via a cannula. Evaporating the benzene solution under vacuum afforded the desired product as a light yellow solid (54 mg, 72% yield). X-ray quality crystals were obtained from a solution of **12** (generated in situ by mixing $\{2,6\text{-}(^iPr_2PO)_2C_6H_3\}Co(PMe_3)_2$ with 1 equiv of Ph_3SnH) in pentane kept at −30 °C. ^1H NMR (400 MHz, C_6D_6, δ): 7.89 (d, $^3J_{H-H}$ = 6.4 Hz, with tin satellites, $^3J_{H-Sn}{}^{117,119}$ = 31.2 Hz, Ar*H* ortho to Sn, 6H), 7.29−7.19 (m, Ar*H*, 6H), 7.19−7.15 (m, Ar*H*, 4H), 6.87 (t, $^3J_{H-H}$ = 7.6 Hz, Ar*H*, 1H), 6.69 (d, $^3J_{H-H}$ = 7.6 Hz, Ar*H*, 2H), 2.62 (heptet, $^3J_{H-H}$ = 7.2 Hz,

https://doi.org/10.1021/acs.inorgchem.4c01993
Inorg. Chem. 2024, 63, 13689−13699

$CH(CH_3)_2$, 2H), 2.26 (heptet, $^3J_{H-H}$ = 7.2 Hz, $CH(CH_3)_2$, 2H), 1.28−1.14 (m, $CH(CH_3)_2$, 12H), 1.13−1.06 (m, $CH(CH_3)_2$, 6H), 1.03 (d, $^2J_{H-P}$ = 6.8 Hz, $P(CH_3)_3$, 9H), 0.91−0.76 (m, $CH(CH_3)_2$, 6H),−15.59 (dt, $^2J_{H-P}$ = 81.2 and 68.0 Hz, with tin satellites, $^2J_{H-Sn}{}^{117,119}$ = 276 Hz, Co*H*, 1H). $^{13}C\{^1H\}$ NMR (101 MHz, C_6D_6, δ): 164.3−163.9 (m, C_2 and C_6 of the pincer unit), 151.8−151.7 (m, Ar*C*), 138.5 (s, with tin satellites, $^2J_{C-Sn}{}^{117,119}$ = 33.2 Hz, Ar*C* in $SnPh_3$), 127.7 (s, Ar*C*), 127.2 (s, with shoulders, Ar*C* in $SnPh_3$), 126.5 (d, J_{C-P} = 3.0 Hz, Ar*C*), 104.7 (td, J = 4.8 and 2.9 Hz, C_3 and C_5 of the pincer unit), 35.3−34.4 (m, $CH(CH_3)_2$), 22.1 (d, $^1J_{C-P}$ = 23.0 Hz, $P(CH_3)_3$), 19.9 (s, $CH(CH_3)_2$), 19.3 (s, $CH(CH_3)_2$), 18.7 (s, $CH(CH_3)_2$), 17.8 (s, $CH(CH_3)_2$); one Ar*C* resonance was not located. $^{31}P\{^1H\}$ NMR (162 MHz, C_6D_6, δ): 209.6 (br, OP^iPr_2, 2P),−6.3 (br, *P*Me$_3$, 1P). $^{119}Sn\{^1H\}$ NMR (149 MHz, C_6D_6, δ):−35.0 (br). Selected ATR-IR data (solid, cm^{-1}): 1951 (ν_{Co-H}). Anal. Calcd for $C_{39}H_{56}O_2P_3SnCo$: C, 56.61; H, 6.82. Found: C, 57.02; H, 6.85.

General Procedure for the Catalytic Hydrostannation Reaction. In a glovebox, {2,6-(^{i}Pr$_2$PO)$_2$C$_6$H$_3$}Co(PMe$_3$)$_2$ (5.0 mg, 9.1 μmol) was transferred into a J. Young NMR tube, after which an alkyne (0.18 mmol) and Ph_3SnH (76 mg, 0.22 mmol, 1.2 equiv) were added sequentially, followed by the addition of C_6D_6 (600 μL). The NMR tube was taken out of the glovebox and placed in a rotary container to protect the reaction from light while ensuring a good mixing. The progress of the reaction was monitored by NMR spectroscopy. To determine the NMR yields for the products, mesitylene (25 μL, 0.18 mmol) was added to the reaction mixture as an internal standard.

X-Ray Structure Determinations. Crystal data collection and refinement parameters are provided in the Supporting Information. The intensity data were collected at 150 K on a Bruker D8 Venture Photon-II diffractometer (**1**, **3**·C_4H_8O, **4**, **10**, and **12**) or Bruker APEX-II CCD diffractometer (**5**) using Mo Kα radiation, λ = 0.71073 Å. The data frames were processed using the program SAINT. The data were corrected for decay, Lorentz, and polarization effects as well as absorption and beam corrections. The structures were solved by a combination of direct methods and the difference Fourier technique as implemented in the SHELX suite of programs and refined by full-matrix least-squares on F^2 for reflections out to 0.75 Å (**1**, **4**, **5**, **10**, and **12**) or 0.80 Å (**3**·C_4H_8O). Nonhydrogen atoms were refined with anisotropic displacement parameters. Hydride ligands were all located directly from the difference map, and their coordinates were refined. The isotropic displacement parameters of the hydrides were refined with the exception of **3**·C_4H_8O and **5**. The remaining hydrogen atoms were calculated and treated with a riding model. The isotropic displacement parameters were defined as a*Ueq (a = 1.5 for methyl, 1.2 for all others) of the adjacent atom. Compound **3** crystallizes as a THF solvate. With the exception of **10**, the crystallographically characterized Co(III) hydride complexes show varying sites and degree of disorder; each was refined with a two-component model. The disorder includes an isopropyl group in **1** and **12**, an isopropyl group and the cocrystallized THF molecule in **3**·C_4H_8O, the *ortho* positions of the pyridyl ring in **4**, and the cyclohexenyl ring in **5**. Crystal structures of **1**, **3**·C_4H_8O, **4**, **5**, **10**, and **12** were deposited at the Cambridge Crystallographic Data Centre (CCDC) and assigned the deposition numbers CCDC 2352515−2352520.

■ ASSOCIATED CONTENT

Supporting Information

The Supporting Information is available free of charge at https://pubs.acs.org/doi/10.1021/acs.inorgchem.4c01993.

Additional experimental details, NMR and IR spectra of the cobalt complexes, and more detailed X-ray crystallographic information (PDF)

Accession Codes

CCDC 2352515−2352520 contain the supplementary crystallographic data for this paper. These data can be obtained free of charge via www.ccdc.cam.ac.uk/data_request/cif, or by emailing data_request@ccdc.cam.ac.uk, or by contacting The Cambridge Crystallographic Data Centre, 12 Union Road, Cambridge CB2 1EZ, U.K.; fax: +44 1223 336033.

■ AUTHOR INFORMATION

Corresponding Author

Hairong Guan − *Department of Chemistry, University of Cincinnati, Cincinnati, Ohio 45221-0172, United States;* orcid.org/0000-0002-4858-3159; Email: hairong.guan@uc.edu

Authors

Sayantani Saha − *Department of Chemistry, University of Cincinnati, Cincinnati, Ohio 45221-0172, United States*

Jeanette A. Krause − *Department of Chemistry, University of Cincinnati, Cincinnati, Ohio 45221-0172, United States*

Complete contact information is available at: https://pubs.acs.org/10.1021/acs.inorgchem.4c01993

Notes

The authors declare no competing financial interest.

■ ACKNOWLEDGMENTS

The authors thank the National Science Foundation (NSF) Chemical Catalysis Program for support of this research project (CHE-2102192) and the NSF MRI Program for support of the instrumentation used in this study, which includes a Bruker D8 Venture diffractometer (CHE-1625737), a Bruker APEX-II CCD diffractometer (CHE-0215950), and a Bruker NEO400 MHz NMR spectrometer (CHE-1726092).

■ REFERENCES

(1) (a) Broere, D. L. J.; Plessius, R.; van der Vlugt, J. I. New Avenues for Ligand-Mediated Processes − Expanding Metal Reactivity by the Use of Redox-Active Catechol, *o*-Aminophenol and *o*-Phenylenediamine Ligands. *Chem. Soc. Rev.* **2015**, *44*, 6886−6915. (b) Singh, K.; Kundu, A.; Adhikari, D. Ligand-Based Redox: Catalytic Applications and Mechanistic Aspects. *ACS Catal.* **2022**, *12*, 13075−13107. (c) Nakada, A.; Matsumoto, T.; Chang, H.-C. Redox-Active Ligands for Chemical, Electrochemical, and Photochemical Molecular Conversions. *Coord. Chem. Rev.* **2022**, *473*, No. 214804.

(2) (a) Pye, D. R.; Mankad, N. P. Bimetallic Catalysis for C−C and C−X Coupling Reactions. *Chem. Sci.* **2017**, *8*, 1705−1718. (b) Powers, I. G.; Uyeda, C. Metal-Metal Bonds in Catalysis. *ACS Catal.* **2017**, *7*, 936−958. (c) Chatterjee, B.; Chang, W.-C.; Jena, S.; Werlé, C. Implementation of Cooperative Designs in Polarized Transition Metal Systems − Significance for Bond Activation and Catalysis. *ACS. Catal.* **2020**, *10*, 14024−14055. (d) Wang, Q.; Brooks, S. H.; Liu, T.; Tomson, N. C. Tuning Metal-Metal Interactions for Cooperative Small Molecule Activation. *Chem. Commun.* **2021**, *57*, 2839−2853.

(3) (a) Li, Y.; Krause, J. A.; Guan, H. Cobalt POCOP Pincer Complexes via Ligand C−H Bond Activation with $Co_2(CO)_8$: Catalytic Activity for Hydrosilylation of Aldehydes in an Open vs a Closed System. *Organometallics* **2018**, *37*, 2147−2158. (b) Li, Y.; Krause, J. A.; Guan, H. Silane Activation with Cobalt on the POCOP Pincer Ligand Platform. *Organometallics* **2020**, *39*, 3721−3730. (c) Li, Y.; Krause, J. A.; Guan, H. POCOP-Type Cobalt and Nickel Pincer Complexes Bearing an Appended Phosphinite Group. *Can. J. Chem.* **2021**, *99*, 147−153.

(4) Timpa, S. D.; Pell, C. J.; Ozerov, O. V. A Well-Defined (POCOP)Rh Catalyst for the Coupling of Aryl Halides with Thiols. *J. Am. Chem. Soc.* **2014**, *136*, 14772−14779.

(5) (a) Choi, J.; MacArthur, A. H. R.; Brookhart, M.; Goldman, A. S. Dehydrogenation and Related Reactions Catalyzed by Iridium Pincer Complexes. *Chem. Rev.* **2011**, *111*, 1761−1779. (b) Haibach, M. C.;

Kundu, S.; Brookhart, M.; Goldman, A. S. Alkane Metathesis by Tandem Alkane-Dehydrogenation−Olefin-Metathesis Catalysis and Related Chemistry. *Acc. Chem. Res.* **2012**, *45*, 947−958. (c) Kumar, A.; Bhatti, T. M.; Goldman, A. S. Dehydrogenation of Alkanes and Aliphatic Groups by Pincer-Ligated Metal Complexes. *Chem. Rev.* **2017**, *117*, 12357−12384.

(6) Hebden, T. J.; St. John, A. J.; Gusev, D. G.; Kaminsky, W.; Goldberg, K. I.; Heinekey, D. M. Preparation of a Dihydrogen Complex of Cobalt. *Angew. Chem., Int. Ed.* **2011**, *50*, 1873−1876.

(7) Baroudi, A.; El-Hellani, A.; Bengali, A. A.; Goldman, A. S.; Hasanayn, F. Calculation of Ionization Energy, Electron Affinity, and Hydride Affinity Trends in Pincer-Ligated d^8-Ir(^{tBu4}PXCXP) Complexes: Implications for the Thermodynamics of Oxidative H_2 Addition. *Inorg. Chem.* **2014**, *53*, 12348−12359.

(8) Foley, B. J.; Palit, C. M.; Timpa, S. D.; Ozerov, O. V. Synthesis of (POCOP)Co(Ph)(X) Pincer Complexes and Observation of Aryl−Aryl Reductive Elimination Involving the Pincer Aryl. *Organometallics* **2018**, *37*, 3803−3812.

(9) The T-shaped, PNP-ligated Co(I) complex also favors the triplet ground state. For details, see: Ott, J. C.; Bürgy, D.; Guan, H.; Gade, L. H. 3d Metal Complexes in T-shaped Geometry as a Gateway to Metalloradical Reactivity. *Acc. Chem. Res.* **2022**, *55*, 857−868.

(10) Xu, G.; Sun, H.; Li, X. Activation of sp^3 Carbon−Hydrogen Bonds by Cobalt and Iron Complexes and Subsequent C−C Bond Formation. *Organometallics* **2009**, *28*, 6090−6095.

(11) (a) Gao, K.; Yoshikai, N. Low-Valent Cobalt Catalysis: New Opportunities for C−H Functionalization. *Acc. Chem. Res.* **2014**, *47*, 1208−1219. (b) Moselage, M.; Li, J.; Ackermann, L. Cobalt-Catalyzed C−H Activation. *ACS Catal.* **2016**, *6*, 498−525. (c) Yoshino, T.; Matsunaga, S. Cobalt-Catalyzed C(sp^3)−H Functionalization Reactions. *Asian J. Org. Chem.* **2018**, *7*, 1193−1205. (d) Gandeepan, P.; Müller, T.; Zell, D.; Cera, G.; Warratz, S.; Ackermann, L. 3d Transition Metals for C−H Activation. *Chem. Rev.* **2019**, *119*, 2192−2452. (e) Baccalini, A.; Vergura, S.; Dolui, P.; Zanoni, G.; Maiti, D. Recent Advances in Cobalt-Catalysed C−H Functionalizations. *Org. Biomol. Chem.* **2019**, *17*, 10119−10141.

(12) (a) Zhang, G.; Vasudevan, K. V.; Scott, B. L.; Hanson, S. K. Understanding the Mechanisms of Cobalt-Catalyzed Hydrogenation and Dehydrogenation Reactions. *J. Am. Chem. Soc.* **2013**, *135*, 8668−8681. (b) Murugesan, S.; Stöger, B.; Weil, M.; Veiros, L. F.; Kirchner, K. Synthesis, Structure, and Reactivity of Co(II) and Ni(II) PCP Pincer Borohydride Complexes. *Organometallics* **2015**, *34*, 1364−1372. (c) Ibrahim, A. D.; Tokmic, K.; Brennan, M. R.; Kim, D.; Matson, E. M.; Nilges, M. J.; Bertke, J. A.; Fout, A. R. Monoanionic Bis(carbene) Pincer Complexes Featuring Cobalt(I-III) Oxidation States. *Dalton Trans.* **2016**, *45*, 9805−9811. (d) Sanjosé-Orduna, J.; Benet-Buchholz, J.; Pérez-Temprano, M. H. Unravelling Molecular Aspects of the Migratory Insertion Step in Cp*Co^{III} Metallacyclic Systems. *Inorg. Chem.* **2019**, *58*, 10569−10577.

(13) (a) Li, J.; Zheng, T.; Sun, H.; Xu, W.; Li, X. Selective C−F/C−H Bond Activation of Fluoroarenes by Cobalt Complex Supported with Phosphine Ligands. *Dalton Trans.* **2013**, *42*, 5740−5748. (b) Lu, F.; Li, J.; Sun, H.; Li, X. Selective C−H Bond Activation of 1,2,4,5-Tetrafluorobenzene by $Co(PMe_3)_4$. *Inorg. Chim. Acta* **2014**, *416*, 222−225. (c) Semproni, S. P.; Hojilla Atienza, C. C.; Chirik, P. J. Oxidative Addition and C−H Activation Chemistry with a PNP Pincer-Ligated Cobalt Complex. *Chem. Sci.* **2014**, *5*, 1956−1960. (d) Roque, J. B.; Shimozono, A. M.; Pabst, T. P.; Hierlmeier, G.; Peterson, P. O.; Chirik, P. J. Kinetic and Thermodynamic Control of C(sp^2)−H Activation Enables Site-Selective Borylation. *Science* **2023**, *382*, 1165−1170. (e) Lee, B.; Pabst, T. P.; Hierlmeier, G.; Chirik, P. J. Exploring the Effect of Pincer Rigidity on Oxidative Addition Reactions with Cobalt(I) Complexes. *Organometallics* **2023**, *42*, 708−718.

(14) (a) Mo, Z.; Chen, D.; Leng, X.; Deng, L. Intramolecular C(sp^3)−H Bond Activation Reactions of Low-Valent Cobalt Complexes with Coordination Unsaturation. *Organometallics* **2012**, *31*, 7040−7043. (b) Zhu, G.; Li, X.; Xu, G.; Wang, L.; Sun, H. A New PC(sp^3)P Ligand and Its Coordination Chemistry with Low-Valent Iron, Cobalt and Nickel Complexes. *Dalton Trans.* **2014**, *43*, 8595−8598. (c) Huang, S.; Zhao, H.; Li, X.; Wang, L.; Sun, H. Synthesis of [POCOP]-Pincer Iron and Cobalt Complexes *via* C_{sp3}−H Activation and Catalytic Application of Iron Hydride in Hydrosilylation Reactions. *RSC Adv.* **2015**, *5*, 15660−15667. (d) Zhu, G.; Wang, L.; Sun, H.; Li, X. Formation of PCP Pincer Cobalt Complexes with Cobaltacycloproprane Moieties *via* Double C_{sp3}−H Bond Activation. *RSC Adv.* **2015**, *5*, 19402−19408. (e) Sun, J.; Luo, L.; Luo, Y.; Deng, L. An NHC−Silyl−NHC Pincer Ligand for the Oxidative Addition of C−H, N−H, and O−H Bonds to Cobalt(I) Complexes. *Angew. Chem., Int. Ed.* **2017**, *56*, 2720−2724.

(15) Klein, H.-F.; Beck, H.; Hammerschmitt, B.; Koch, U.; Koppert, S.; Cordier, G.; Paulus, H. Synthesis, Properties, and Structure of a Dinitrogen Bridged Dinuclear Hydridocobalt Complex and Its Reactions with 1-Alkynes. *Z. Naturforsch., B: J. Chem. Sci.* **1991**, *46*, 147−156.

(16) Yoshimitsu, S.; Hikichi, S.; Akita, M. Synthesis and Characterization of Coordinatively Unsaturated Alkynyl- and Aryl-Cobalt Complexes with 15 Valence Electrons, Tp^{iPr2}Co−R, Bearing the Hydrotris(3,5-diisopropylpyrazolyl)borato Ligand (Tp^{iPr2}). *Organometallics* **2002**, *21*, 3762−3773.

(17) Bianchini, C.; Peruzzini, M.; Vacca, A.; Zanobini, F. Metal−Hydride Alkynyl → Metal−Vinylidene Rearrangements Occurring in both Solid State and Solution. Role of the 1-Alkyne Substituent in Determining the Relative Stability of π-Alkyne, Hydride Alkynyl, and Vinylidene Forms at Cobalt. *Organometallics* **1991**, *10*, 3697−3707.

(18) Basallote, M. G.; Hughes, D. L.; Jiménez-Tenorio, M.; Leigh, G. J.; Vizcaíno, M. C. P.; Jiménez, P. V. Chemistry of Cobalt Complexes with 1,2-Bis(diethylphosphino)ethane: Hydrides, Carbon Disulfide Complexes, and C−H Cleavage in Activated Alk-1-ynes. Crystal Structure of $[CoH(C{\equiv}CCO_2Et)(Et_2PCH_2CH_2PEt_2)_2][BPh_4]$. *J. Chem. Soc., Dalton Trans.* **1993**, 1841−1847.

(19) (a) Beattie, J. W.; Wang, C.; Zhang, H.; Krogman, J. P.; Foxman, B. M.; Thomas, C. M. Dimerization of Terminal Alkynes Promoted by a Heterobimetallic Zr/Co Complex. *Dalton Trans.* **2020**, *49*, 2407−2411. (b) Hunter, N. H.; Lane, E. M.; Gramigna, K. M.; Moore, C. E.; Thomas, C. M. C−H Bond Activation Facilitated by Bis(phosphinoamide) Heterobimetallic Zr/Co Complexes. *Organometallics* **2021**, *40*, 3689−3696.

(20) Ventre, S.; Derat, E.; Amatore, M.; Aubert, C.; Petit, M. Hydrido-Cobalt Catalyst as a Selective Tool for the Dimerisation of Arylacetylenes: Scope and Theoretical Studies. *Adv. Synth. Catal.* **2013**, *355*, 2584−2590.

(21) Chang, W.-C.; Randel, H.; Weyhermüller, T.; Auer, A. A.; Farès, C.; Werlé, C. A Cooperative Rhodium/Secondary Phosphine Oxide [Rh/P(O)nBu$_2$] Template for Catalytic Hydrodefluorination of Perfluoroarenes. *Angew. Chem., Int. Ed.* **2023**, *62*, No. e202219127.

(22) The Co−P and Co−C_{ipso} bond lengths are also almost identical. For details, see Supporting Information.

(23) The NMR resonances for the alkynyl carbons that are directly attached to cobalt were not located. This is due to the broadening caused by the quadrupolar ^{59}Co nucleus coupled by extensive splitting by the ^{31}P nuclei.

(24) Zhang, J.; Adhikary, A.; King, K. M.; Krause, J. A.; Guan, H. Substituent Effects on Ni−S Bond Dissociation Energies and Kinetic Stability of Nickel Arylthiolate Complexes Supported by a Bis(phosphinite)-based Pincer Ligand. *Dalton Trans.* **2012**, *41*, 7959−7968.

(25) Giordan, J. C. Negative Ions: Effect of α- vs. β-Silyl Substitution on the Negative Ion States of π Systems. *J. Am. Chem. Soc.* **1983**, *105*, 6544−6546.

(26) (a) Castarlenas, R.; Di Giuseppe, A.; Pérez-Torrente, J. J.; Oro, L. A. The Emergence of Transition-Metal-Mediated Hydrothiolation of Unsaturated Carbon−Carbon Bonds: A Mechanistic Outlook. *Angew. Chem., Int. Ed.* **2013**, *52*, 211−222. (b) Beletskaya, I. P.; Ananikov, V. P. Transition-Metal-Catalyzed C−S, C−Se, and C−Te Bond Formations via Cross-Coupling and Atom-Economic Addition Reactions. Achievements and Challenges. *Chem. Rev.* **2022**, *122*, 16110−16293.

https://doi.org/10.1021/acs.inorgchem.4c01993
Inorg. Chem. 2024, 63, 13689−13699

(27) (a) Lang, R. F.; Ju, T. D.; Kiss, G.; Hoff, C. D.; Bryan, J. C.; Kubas, G. J. Oxidative Addition of Thiols, Disulfides, Iodine, and Hydrogen Iodide to $W(CO)_3(P^iPr_3)_2$. Preparation of Stable 17-Electron Tungsten Thiolate Radicals from Complexes with Weak W−H Bonds. *J. Am. Chem. Soc.* **1994**, *116*, 7917−7918. (b) Lang, R. F.; Ju, T. D.; Bryan, J. C.; Kubas, G. J.; Hoff, C. D. Oxidative Addition of Thiols, and Thiol/Thiolate Exchange Reactions of Low Valent Molybdenum and Tungsten Complexes. Synthetic, Structural and Calorimetric Study of Trigonal Prismatic $W(CO)_2$(1,10-phenanthroline)(3,4-toluenedithiolate). *Inorg. Chim. Acta* **2003**, *348*, 157−164. (c) Nakata, N.; Yamamoto, S.; Hashima, W.; Ishii, A. Synthesis and X-ray Structural Analysis of Hydrido(thiolato) Platinum(II) Complexes. *Chem. Lett.* **2009**, *38*, 400−401.

(28) (a) Wang, L.-S.; McDonald, R.; Cowie, M. S−H Bond Activation in H_2S and Thiols by $[RhMn(CO)_4(Ph_2PCH_2PPh_2)_2]$. Compounds Containing Terminal or Bridging Sulfhydryl and Thiolato Groups. *Inorg. Chem.* **1994**, *33*, 3735−3744. (b) Khorasani-Motlagh, M.; Safari, N.; Pamplin, C. B.; Patrick, B. O.; James, B. R. Oxidative Addition of Thiols to $(CO)_3Mo(\mu$-dppm$)_2Ru(CO)_3$ with Formation of Hydrido, Bridged-Thiolate Complexes (dppm = $Ph_2PCH_2PPh_2$). *Inorg. Chim. Acta* **2010**, *363*, 779−783.

(29) Jennings, M. C.; Puddephatt, R. J. Oxidative Addition of Thiols to a Coordinatively Unsaturated Triplatinum Cluster Complex. *Inorg. Chem.* **1988**, *27*, 4280−4284.

(30) Jiao, G.; Li, X.; Sun, H.; Xu, X. Synthesis and Reactivity of a Novel Hydridocobalt(III) Complex Containing Trimethylphosphine and Thiophenolato Ligands. *J. Organomet. Chem.* **2007**, *692*, 4251−4258.

(31) Niu, Q.; Sun, H.; Li, X.; Klein, H.-F.; Flörke, U. Synthesis and Catalytic Application in Hydrosilylation of the Complex *mer*-Hydrido(2-mercaptobenzoyl)tris(trimethylphosphine)cobalt (III). *Organometallics* **2013**, *32*, 5235−5238.

(32) Xu, H.; Williard, P. G.; Bernskoetter, W. H. C−H Bond Activation and S-atom Transfer from Cobalt(III) Thiolate and Isothiocyanate Complexes. *Dalton Trans.* **2014**, *43*, 14696−14700.

(33) Poitras, A. M.; Bezpalko, M. W.; Foxman, B. M.; Thomas, C. M. Cooperative Activation of O−H and S−H Bonds across the Co−P Bond of an *N*-heterocyclic Phosphido Complex. *Dalton Trans.* **2019**, *48*, 3074−3079.

(34) (a) Zhang, J.; Medley, C. M.; Krause, J. A.; Guan, H. Mechanistic Insights into C−S Cross-Coupling Reactions Catalyzed by Nickel Bis(phosphinite) Pincer Complexes. *Organometallics* **2010**, *29*, 6393−6401. (b) Chakraborty, S.; Zhang, J.; Patel, Y. J.; Krause, J. A.; Guan, H. Pincer-Ligated Nickel Hydridoborate Complexes: the Dormant Species in Catalytic Reduction of Carbon Dioxide with Boranes. *Inorg. Chem.* **2013**, *52*, 37−47. (c) Hao, J.; Mougang-Soumé, B.; Vabre, B.; Zargarian, D. On the Stability of a $POC_{sp3}OP$-Type Pincer Ligand in Nickel(II) Complexes. *Angew. Chem., Int. Ed.* **2014**, *53*, 3218−3222.

(35) (a) Piana, H.; Kirchgäßner, U.; Schubert, U. Übergangsmetall-Stannyl-Komplexe, Metall, Wasserstoff, Zinn-Dreizentrenbindung bei Hydrido-Stannyl-Komplexen der 6. *Nebengruppe. Chem. Ber.* **1991**, *124*, 743−751. (b) Trebbe, R.; Schager, F.; Goddard, R.; Pörschke, K.-R. *cis*-$(R'_2PC_2H_4PR'_2)PdH(SnR_3)$ Complexes: Trapped Intermediates in the Palladium-Catalyzed Hydrostannation of Alkynes. *Organometallics* **2000**, *19*, 521−526. (c) Adams, R. D.; Fang, F.; Smith, M. D.; Zhang, Q. The Reactions of $Ir(CO)Cl(PPh_3)_2$ with $HSnPh_3$. *J. Organomet. Chem.* **2011**, *696*, 2904−2909.

(36) Winterhalter, U.; Zsolnai, L.; Kircher, P.; Heinze, K.; Huttner, G. Reductive Activation of Tripod Cobalt Compounds: Oxidative Addition of H−H, P−H, and Sn−H Functions. *Eur. J. Inorg. Chem.* **2001**, *2001*, 89−103.

(37) Roddick, D. M. Tuning of PCP Pincer Ligand Electronic and Steric Properties. *Top. Organomet. Chem.* **2013**, *40*, 49−88.

(38) Zhu, J.; Lin, Z.; Marder, T. B. Trans Influence of Boryl Ligands and Comparison with C, Si, and Sn Ligands. *Inorg. Chem.* **2005**, *44*, 9384−9390.

(39) (a) Smith, N. D.; Mancuso, J.; Lautens, M. Metal-Catalyzed Hydrostannations. *Chem. Rev.* **2000**, *100*, 3257−3282. (b) Alami, M.; Hamze, A.; Provot, O. Hydrostannation of Alkynes. *ACS Catal.* **2019**, *9*, 3437−3466. (c) Roberts, D. D.; McLaughlin, M. G. Strategies for the Controlled Hydrostannylation of Alkynes. *Eur. J. Org. Chem.* **2023**, *26*, No. e202300755.

(40) (a) Kikukawa, K.; Umekawa, H.; Wada, F.; Matsuda, T. Regioselective Hydrostannation of Terminal Acetylenes. *Chem. Lett.* **1988**, *17*, 881−884. (b) Ghosh, B.; Maleczka, R. E., Jr. Ni, Co, and Mo-catalyzed Alkyne Hydrostannations Using Bu_3SnCl/PMHS/KF/18-crown-6 as an in situ Bu_3SnH Source. *Tetrahedron Lett.* **2011**, *52*, 5285−5287.

(41) 4-Ethynylanisole was chosen as the alkyne simply because the ^1H NMR resonances for the three hydrostannation products are well separated in the aromatic region.

(42) Wile, B. M.; McDonald, R.; Ferguson, M. J.; Stradiotto, M. Synthesis and Reactivity of New κ^2-[*P*,*N*]Pt(II) Complexes of Diisopropylphosphino-Substituted 2-Dimethylaminoindene. *Organometallics* **2005**, *24*, 1959−1965.

(43) Leusink, A. J.; Budding, H. A.; Marsman, J. W. Studies in Group IV Organometallic Chemistry XXIV. Structure of Products Obtained in the Hydrostannation of Ethynes. *J. Organomet. Chem.* **1967**, *9*, 285−294.

(44) Phosphines can form Lewis adducts with Sn(IV) compounds, although the tin center is often more Lewis acidic than that in Ph_3SnH. For examples, see: (a) Liang, L.-C.; Chang, Y.-N.; Chen, H.-S.; Lee, H. M. Biphenolate Phosphine Complexes of Tin(IV). *Inorg. Chem.* **2007**, *46*, 7587−7593. (b) King, R. P.; Woodward, M. S.; Grigg, J.; McRobbie, G.; Levason, W.; Reid, G. Tin(IV) Fluoride Complexes with Neutral Phosphine Coordination and Comparisons with Hard N- and O-Donor Ligands. *Dalton Trans.* **2021**, *50*, 14400−14410.

(45) Rossi-Ashton, J. A.; Clarke, A. K.; Unsworth, W. P.; Taylor, R. J. K. Phosphoranyl Radical Fragmentation Reactions Driven by Photoredox Catalysis. *ACS Catal.* **2020**, *10*, 7250−7261.

(46) (a) Cheng, L.-J.; Mankad, N. P. Heterobimetallic Control of Regioselectivity in Alkyne Hydrostannylation: Divergent Syntheses of α- and (*E*)-β-Vinylstannanes via Cooperative Sn−H Bond Activation. *J. Am. Chem. Soc.* **2019**, *141*, 3710−3716. (b) Liu, J.; Song, H.; Wang, T.; Jia, J.; Tong, Q.-X.; Tung, C.-H.; Wang, W. Iron-Catalyzed Regiodivergent Hydrostannation of Alkynes: Intermediacy of Fe(IV)−H versus Fe(II)−Vinylidene. *J. Am. Chem. Soc.* **2021**, *143*, 409−419.

(47) Ventre, S.; Simon, C.; Rekhroukh, F.; Malacria, M.; Amatore, M.; Aubert, C.; Petit, M. Catalytic Version of Enediyne Cobalt-Mediated Cycloaddition and Selective Access to Unusual Bicyclic Trienes. *Chem.—Eur. J.* **2013**, *19*, 5830−5835.

https://doi.org/10.1021/acs.inorgchem.4c01993
Inorg. Chem. 2024, 63, 13689−13699